

## PDF hosted at the Radboud Repository of the Radboud University Nijmegen

The following full text is a publisher's version.

For additional information about this publication click this link.

<http://hdl.handle.net/2066/35610>

Please be advised that this information was generated on 2019-12-13 and may be subject to change.

# Molecular characterization of Sin3 PAH-domain interactor specificity and identification of PAH partners

Xavier Le Guezennec, Michiel Vermeulen and Hendrik G. Stunnenberg\*

Department of Molecular Biology, NCMLS, Radboud University Nijmegen, PO Box 9101, 6500 HB Nijmegen, The Netherlands

Received December 21, 2005; Revised June 19, 2006; Accepted July 13, 2006

## ABSTRACT

**Sin3 is the central component of a multisubunit co-repressor complex. A number of DNA-binding proteins are targeted by the Sin3 complex to chromatin through association with its paired amphipathic helix (PAH) domains. Here, we performed a yeast two-hybrid screening using a peptide aptamer library and identified peptides that interact with either PAH1 or PAH2. Analysis of PAH2 interacting peptides uncovered motifs similar to previously characterized PAH2 interacting proteins, Mad, Ume6 and kruppel-like members, while analysis of PAH1 interacting peptides revealed an LXXLL motif. In addition, a tandem affinity purification (TAP)-tagging approach of Sin3b resulted in the isolation of known and novel interactors amongst which neural retina leucine (NRL) zipper. Strikingly, one of the identified PAH2 interacting peptide showed strong resemblance to the NRL region amino acids 125–150. Direct association between PAH2 and NRL was shown and NRL(125–150) mediated transcriptional repression in reporter assays. Finally, we reveal that PAH1 and PAH2 amino acids 7, 14 and 39 shown previously to be important for Mad–PAH2 interaction, also play an important role in the specificity of interaction between PAH1, PAH2 and identified aptamers. Our results provide novel insights into the molecular determinant of the specificity of PAH1 and PAH2 for their interacting partners.**

## INTRODUCTION

Transcriptional regulation is central to many cellular functions including differentiation and development. In eukaryotes, alteration of chromatin structure plays an integral role in gene regulation. Such chromatin changes occur on core

histone tails at a post-translational level and are induced by different classes of enzymes including histone acetyl transferases (HAT) or histone deacetylases (HDAC) (1,2). Recruitment of HAT complexes to genes generally results in transcription activation while recruitment of HDACs results in transcriptional repression (3,4). The Sin3 protein is an evolutionary conserved repressor that is part of ~1.2 MDa multi-protein co-repressor complex associated with HDAC activity. The core subunits of the Sin3 complex include HDAC1, HDAC2, RbAp46/48, RBP1, SAP130, BRMS1, SDS3, SAP30 and SAP18 (5–11).

Sin3 contains four conserved imperfect repeats of ~100 amino acids termed paired amphipathic helix (PAH) domains which are protein–protein interaction modules for an array of DNA-binding transcriptional repressors (12). PAH1 has been reported so far to interact with Opi1, Pfl1, NRSF, N-CoR and SMRT (13–17). The PAH2 domain covers a broad range of interactions including Mad protein family members, Sp1-like repressor proteins, HBP1, Pfl1 and yeast Ume6 (14,18–23).

The interaction of Sin3 with the tumour suppressor Mad is particularly well studied. The ability of Mad to inhibit cell proliferation and to repress transcription is dependent on an N-terminal N<sup>8</sup>IQMLLEAADYLE<sup>20</sup> domain named SID (Sin3 interacting domain) (22,24). In nuclear magnetic resonance experiments, Mad SID folds as an amphipathic helix and contacts the PAH2 domain of Sin3 which folds as a four-helix bundle (25–27). A recent study from Swanson *et al.* (23) revealed a reverse N-terminal to C-terminal orientation of the HBP1 SID amphipathic helix in contact with PAH2 as compared with the Mad SID. Furthermore, molecular dynamic simulation has suggested that TIEG2 SID binds PAH2 in a different orientation than the Mad SID, suggesting multiple ways to interact with PAH2 (23,28).

Initial attempts to identify a SID consensus sequences for Mad family members revealed the following degenerated sequence:  $\phi$ ZZ $\phi$  $\phi$ XAAXX $\phi$ nXXn with X for any non-proline residues,  $\phi$  for bulky hydrophobic residues and n for negatively charged residues (25–27). Other studies have reported the SID of SPI-like members with PAH2 as  $\phi$  $\phi$ XAAXX $\phi$ . Despite a wealth of information on PAH2 and interacting

\*To whom correspondence should be addressed. Tel: +31 3610524; Fax: +31 3610520; Email: h.stunnenberg@ncmls.ru.nl

SIDs, PAH1 remains poorly characterized and the identification of a PAH1 interaction motif has not been reported.

Here, we screened peptide aptamer libraries to identify PAH1 and PAH2 interacting peptides. Different motifs interacting with PAH1 and PAH2 are presented. We show that binding of the identified aptamers to the PAH1 or PAH2 domains is affected by PAH1 and PAH2 mutations shown previously to be important for an interaction with the Mad SID (29). A complementary approach using TAP-tagging of mSin3b revealed the transcription factor NRL, a neural retina leucine zipper protein which contains an amino acid sequence similar to one of the PAH2 aptamers, in addition to proteins that are part of the core Sin3/HDAC complex.

## MATERIALS AND METHODS

### Cloning and binding assay

Oligos containing a BamHI restriction site overhang followed by P1-1 EGDWLFVLLVGLL or P1-8 SAAMGSAEFEALVALLFLSEE encoding sequences and an EcoRI restriction site overhang were annealed, phosphorylated and ligated in frame to the GB1 domain of streptococcal protein G using BamHI and EcoRI site of pGEV2 plasmid. A fragment encompassing mSin3b was subcloned from pvzmSin3b (20) into EcoRI and BamHI site from pZNX. pZNX has been described in another study and contains one ProtA domain, two TEV cleavage sites and an myc epitope. NRL was amplified by PCR from plasmid pcDNA4-NRL using a forward primer containing an EcoRI restriction site overhang with a myc tag (MEQKLISEEDL) in combination with a reverse primer containing a BamHI restriction site and after digestion by EcoRI/BamHI was ligated into pSG5 (Stratagene) (30). NRL was also amplified with a forward primer containing an EcoRI restriction site overhang in combination with a reverse primer containing an HindIII restriction site overhang and after digestion by EcoRI/HindIII, the digested product was ligated into PM to generate a GAL4 fusion protein with NRL. NRL SID was generated by annealing oligos containing an EcoRI site overhang followed by HVQLAERFS-DAALSMSVRELNR encoding sequence and an HindIII restriction site overhang. After annealing and phosphorylation, NRL SID was ligated in frame to GAL4 of PM plasmid to generate PM-NRL SID. All constructs and positive aptamers vectors were validated by DNA sequencing.

The P1-1 and P1-8 or mutant aptamers fused to the GB1 domain of streptococcal protein G was prepared as described previously (25). GST-PAH1 (amino acids 34–108) and GST-PAH2 (amino acids 148–252) and their respective mutants at position 7, 14 and 39 were expressed and purified as described previously (31).

GST-PAH1 or PAH2 (10  $\mu$ g) and their respective mutants were incubated with protG-P1-1 or protG-P1-8 and bound to IgG-Sepharose (Pharmacia) in 150 mM NaCl, 0.1% NP-40 and 20 mM Tris (pH 7.6). Beads were washed three times with the same buffer. Bound proteins were eluted with 0.1 M glycine (pH 2.6), separated by SDS gel electrophoresis and stained using coomassie blue.

mycNRL (40  $\mu$ g) was transfected in 293 HEK (human embryonic kidney) cells on a 14 cm dish using the calcium phosphate method. Whole-cell extract was prepared 36 h

after transfection as described previously (32). Subsequently, extracts were incubated in 3 vol of IPP150 (10 mM Tris, 150 mM NaCl, 0.1% NP-40 and 0.5 mM EDTA) and equal amounts (2  $\mu$ g) of GST-PAH1 or GST-PAH2 and GST-Sepharose 4B (Amersham). After 1 h incubation at 4°C on a rotating wheel, beads were washed three times with 20 beads volumes of IPP150. Bound fraction was subjected to SDS-PAGE and western blotting using  $\alpha$ -myc monoclonal antibody (9E10).

### Reporter assays

Transfection was performed in 293 HEK cells using Lipofectamine 2000 according to the manufacturer's protocol (Invitrogen). pGL5, a firefly luciferase reporter plasmid (400 ng), under the control of five GAL4-binding sites and pRL-tk (Promega) (400 ng), a *Renilla* luciferase control plasmid, was cotransfected with either PM (GAL4 DBD plasmid; 3  $\mu$ g) or PM-NRL (3  $\mu$ g) and PM-NRL SID (3  $\mu$ g). Total amount of DNA was adjusted to 4  $\mu$ g with pBS plasmid (Stratagene). The cells were harvested 48 h after transfection. Lysis and measurement of *Renilla* and firefly luciferase activities were performed with the dual-Luciferase<sup>®</sup> Reporter assay system according to the manufacturer's protocol (Promega). The 293 HEK cells were treated with trichostatin A (TSA; 100 ng/ml) 24 h before harvesting.

### Yeast two-hybrid screening

Yeast strain KF1 (*MATa trp1-901, leu2-3,112 his3-200 gal4 $\Delta$  gal80 $\Delta$  LYS2::GAL1-HIS3 GAL2-ADE2 met2::GAL7-lacZ SPAL10-URA3*) was used for the screening. As a bait the PAH1 or the PAH2 domain of mSin3b were fused in frame with the GAL4 DNA-binding domain in vector pcp97 described previously (29). The yeast prey vector padTRX encodes the *Escherichia coli* thioredoxin A (trxA) gene fused to the Gal4 activation domain. The 20 amino acid randomized peptide library was inserted in the RsrII site of trxA which corresponds to a constrain loop and was estimated to be of a complexity of  $2 \times 10^8$  individual members (33). KF1 containing a PAH1 or PAH2 bait was transformed using LiAC method with the peptide aptamer expression library and was first selected for growth on media lacking adenine. Subsequently KF1 positive transformants were replicas plated on media lacking histidine in the presence of increasing concentration of the inhibitor 3-amino-triazole (3AT) as indicated.

After rescue of the positive aptamer expression vectors, the PAH binding specificity was established in the *Saccharomyces cerevisiae* Y190 (Clontech) strain using PAH1 and PAH2 mutants as described previously (29). Quantitative  $\beta$ -galactosidase assay was performed using *O*-nitrophenyl  $\beta$ -D-galactopyranoside (ONPG) as a substrate. Fresh transformants were grown overnight in 5 ml SD-leu-trp selective culture medium; 1.5 ml cells were concentrated five times in buffer Z (60 mM Na<sub>2</sub>HPO<sub>4</sub>, 60 mM NaH<sub>2</sub>PO<sub>4</sub>, 10 mM KCl and 1 mM MgSO<sub>4</sub>, pH 7.0). Cells were resuspended in 100  $\mu$ l buffer Z and freeze thawed. Buffer Z (0.7 ml) supplemented with 50 mM  $\beta$ -mercaptoethanol and 160  $\mu$ l (4 mg/ml) ONPG was added to initiate the reaction. Incubations for 30 min up to 2 h were performed at 30°C. Reactions were stopped with 0.4 ml of 1 M Na<sub>2</sub>CO<sub>3</sub>.  $\beta$ -Galactosidase units

were calculated according to the formula  $\beta$ -galactosidase units ( $\mu\text{mol ONPG} \times \text{min}^{-1}$ ) =  $1000 \times \text{OD}_{420}/(\text{time in min} \times 0.1 \times 5 \times \text{OD}_{600})$ . Experiments were repeated at least three times and in triplicate.

## RESULTS

### Identification of PAH1 and PAH2 aptamers

The PAH2 domain of Sin3 associates with a number of proteins and the interaction domains determine a tentative consensus SID. A PAH1 interaction consensus has, however, not been determined. Therefore, we performed a peptide library screen to identify specific PAH1 and PAH2 interacting peptides. We screened a random constrained 20mer peptide library displayed on the active site loop of *E. coli* thioredoxin (TRX) molecule fused to the Gal4 transcription activation domain in a yeast two-hybrid assay. The PAH1 or the PAH2 domain of mSin3b were fused to the DNA-binding domain of Gal4 (G4DBD) and used as baits. Interaction between baits and preys yields transactivation of the reporter gene *GAL1-HIS3* and consequent growth on media lacking histidine. The relative strength of the interaction was assessed by determining resistance to the histidine biosynthesis inhibitor 3-amino-triazole (3AT). As a control prey, we used the previously described Mad SID (G4AD-TRX-Mad) known to specifically interact with PAH2 (29). Mad SID combined with PAH2 supported growth of yeast on media lacking histidine and supplemented with 50 mM 3AT whereas Mad SID combined with PAH1 did not support growth. Thus, Mad specifically interacts with PAH2 in this assay (Figure 1A). Screening  $10^6$  and  $2 \times 10^6$  transformed yeast clones for PAH1 and PAH2 interactors led to the isolation of 8 and 11 different transformants, respectively (Figure 1A and B). Transformants showed growth in the presence of 50 mM up to 100 mM 3AT for PAH1 aptamers and from 10 mM up to 100 mM 3AT for PAH2 aptamers. After isolation of the prey plasmid, the sequence of the peptide insert was determined (Table 1).

### The FXXLVXLL motif is a PAH1 interacting motif

To characterize the identified PAH1 aptamers we first analysed their specificity. We retransformed each prey with PAH2 or PAH1 in YN1 yeast strain and performed quantitative  $\beta$ -galactosidase assay. Background levels were observed for every PAH1 aptamer in combination with G4DBD-PAH2, showing that interaction between PAH1 recovered aptamers and PAH1 was specific (Figure 2A).

We reported previously that introduction of PAH2 residues Phe7, Val14 and Gln39 at their corresponding position in PAH1 enables a specific interaction with Mad, a PAH2 specific interacting protein and showed that PAH2 residues Phe7, Val14 and Gln39 play an important role in determining the specificity of the PAH2-Mad interaction. Assuming that amino acids at the respective position in PAH1 play a similar role in determining the specificity between PAH1 and PAH1 aptamers, we hypothesized PAH1 residues Val7, Leu14 and Lys39 to be specific molecular determinants of PAH1-PAH1 aptamers interaction. To test this assumption, we assessed whether binding of the aptamers to PAH1 was

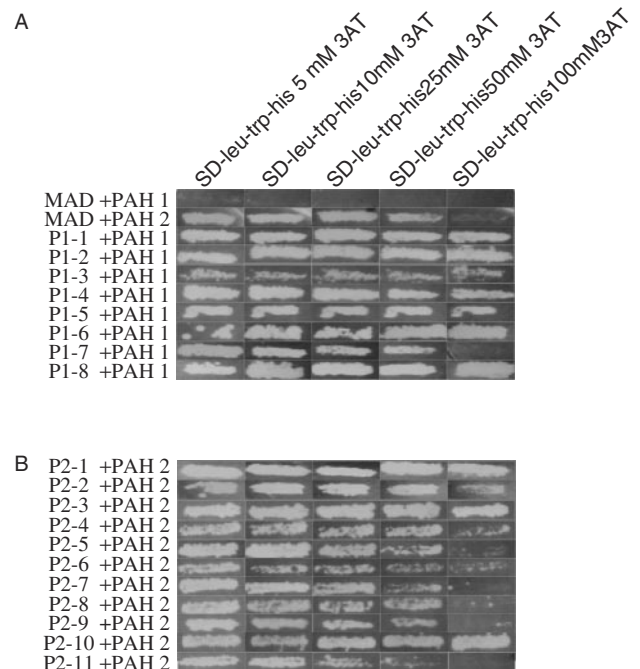


**Figure 1.** Identification of aptamers interacting with the PAH1 or the PAH2 domain of mSin3b in a yeast two-hybrid screen. Yeast containing a control Mad1 SID sequence (5–24) fused to GAL4AD in combination with PAH2 fused to Gal4DBD is able to survive on media lacking histidine with 50 mM 3AT while yeast containing Mad1 and PAH1 fused to G4DBD was not able to support growth. Yeast containing PAH1 aptamers (P1-1–P1-8) (A) with a G4DBD-PAH1 or PAH2 aptamers (P2-1–P2-11) (B) with a G4DBD-PAH2 (B) survived on media lacking histidine supplemented with at least 50 mM 3AT.

**Table 1.** Sequence of peptide aptamers identified from a screening with a G4DBD-PAH1 or G4DBD-PAH2 bait

Aptamers binding to the PAH1 domain of mSin3b	
P1-1	EGDWLFFVLLVGLL <sup>a</sup>
P1-2	LACRCWRCVHTRVRLLLW <sup>a</sup>
P1-3	VDVYGSFGLLWCFCFVSEC
P1-4	LWLLSEVSSVYGT <sup>a</sup>
P1-5	SLALYASIWLLAEHWPQGLI
P1-6	WSLTWVPLYVLTMCAYWRSL
P1-7	DRLSFCWCWWLVFLTHHAAG
P1-8	AAMGSAEFEALVALLFLCEE
Aptamers binding to the PAH2 domain of mSin3b	
P2-1	NLGLLVLGSVCTFRLGLL <sup>a</sup>
P2-2	VDSAWAALLSVACCSLWGLV
P2-3	EGCVVDWAAWLVLYGYAAGW
P2-4	MPSSLNFGSFMGASLWGPLVIAFFLFRFRRTGLFLLVWV <sup>a</sup>
P2-5	WWAWLSVKLGHSGDWLVSLF
P2-6	VVFLCFLDSLSCAVDAAGDD
P2-7	GVFFVLLWTSMPAESTSM
P2-8	SSPYCSSRWKILSF <sup>a</sup>
P2-9	FYLWMLSRGGSGPMLLQIVL
P2-10	CMWLMGHSMRLLIWCACMT
P2-11	VEHCDFCCTVAALVLMRES

<sup>a</sup>Indicates a truncated peptide.

affected by mutating the amino acid Val7 and Leu14 into Phe7 and Val14, respectively, as they appear in PAH2. All PAH1 aptamers except P1-4 showed complete loss of interaction upon mutation of L14V; aptamers that interacted weakly with PAH1 were also strongly affected by the V7F mutation

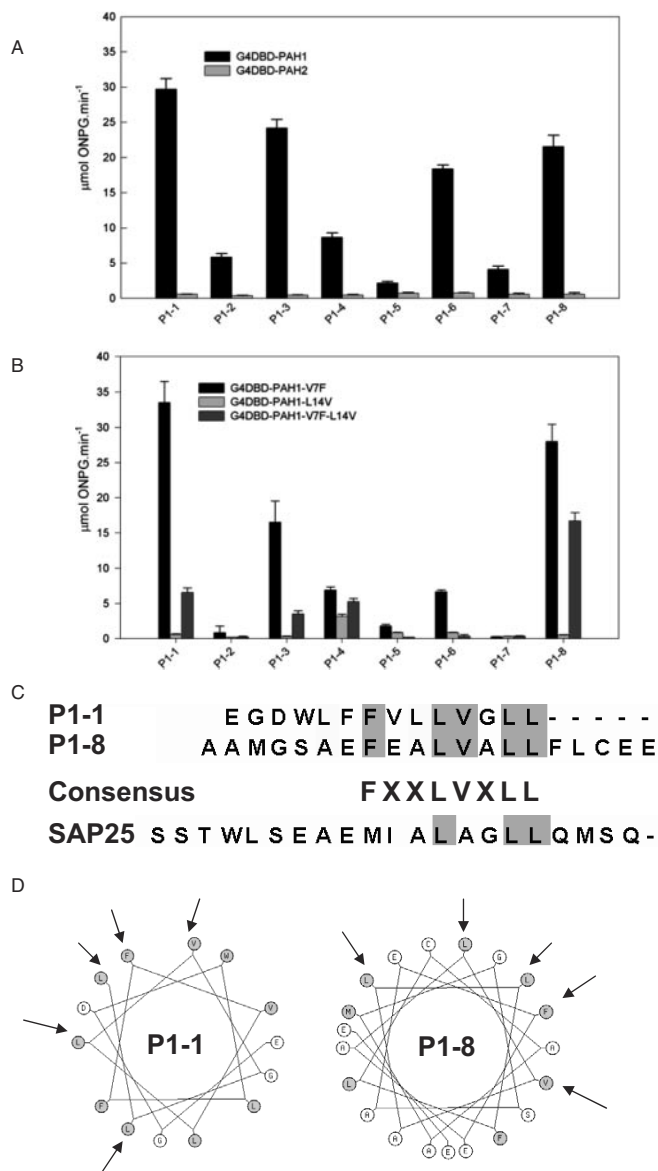


**Figure 2.** Analysis of the interaction of PAH1 aptamers *in vitro*. (A) PAH1 aptamers fused to G4AD were assayed in liquid culture to examine  $\beta$ -galactosidase activity either in the presence G4DBD fused to PAH1 and PAH2. (B)  $\beta$ -Galactosidase assay of PAH1 aptamers in the presence of G4DBD fused to PAH1 single or double mutant V7F and L14V. (C) Sequence alignment of P1-1 and P1-8 showing conservation of an FXXLVXLL motif with SAP25. (D) Helical wheel of P1-1 and P1-8. Arrows depict FXXLVXLL residues localized within one side of the helix in P1-1 or P1-8.

(Figure 2B). Despite an impaired interaction of PAH1 L14V with PAH1 aptamers, PAH1 V7F L14V double mutant readily associated with PAH1 aptamers suggesting that in a double mutant context, V7F mutation partially suppressed the critical effect of L14V mutation. We conclude that PAH1 Leu14 is a critical residue for binding of PAH1 aptamers in our yeast two-hybrid assay.

P1-1 and P1-8 boosted relatively high levels of the reporter gene activity and inspection of the amino acid sequence revealed the shared motif FXXLVXLL (Figure 2C). Secondary structure prediction showed a preference for P1-1

and P1-8 to adopt an  $\alpha$ -helix and a helical wheel projection showed that the FXXLVXLL motif is placed on one surface of the  $\alpha$ -helix. Such a structural characteristic has also been described in the SID of Mad family members that bind PAH2 (Figure 2D).

To corroborate and validate the interaction between PAH1 and P1-1 or P1-8, *in vitro* pull-down assay was performed. We expressed and purified a fusion protein consisting of the ProtG domain followed by P1-1 or P1-8 that was incubated with IgG beads in the presence of GST-PAH1, GST-PAH2 or GST-PAH1 mutants. A direct interaction with PAH1 but not PAH2 was observed, thus confirming the PAH1 domain specificity of the aptamers (Figure 3A). The L14V point mutation in PAH1 impaired binding to P1-1 and P1-8 while a modest decrease in binding was observed with V7F, confirming and extending the yeast two-hybrid observations. Furthermore substitution of Lys39 in PAH1 with Gln39, the amino acid present in PAH2 on that position, abolished the interaction with P1-1 and P1-8. As observed previously in yeast two-hybrid experiments, PAH1 V7F L14V double mutants interacted with P1-1 and P1-8 in contrast to PAH1 L14V single mutant which did not associate with P1-1 and P1-8. This subtle difference suggests that in a PAH1 V7F L14V context, PAH1 V7F mutation suppressed the critical effect of PAH1 L14V mutation. Double mutant V7F K39Q and triple mutant V7F L14V K39Q did not associate with either P1-1 or P1-8. We conclude that Leu14 and Lys39 in PAH1 are critical amino acids for interaction while Val7 may only have a stabilizing role.

To establish the importance of the proposed FXXLVXLL motif for an interaction with PAH1, an alanine scan of P1-8 was performed on the presumed conserved residues of the postulated motif and tested in IgG pull-down assay with GST-PAH1 (Figure 3B and C). Mutating Leu15 or Leu16 severely destabilized the interaction between the motif and PAH1 while mutating Leu12 significantly enhanced binding. Mutating Phe9 or Val13 displayed only minor effects. Therefore Leu15 and Leu16 in P1-8 are critical for interacting with PAH1 whereas Leu12 can be mutated into an alanine to increase *in vitro* binding of P1-8 to PAH1.

Consistent with our findings a recent study described a novel PAH1 interacting protein, SAP25, a component of the Sin3 complex with a LXXLL motif that is also present in the PAH1 aptamers P1-1 and P1-8 (Figure 2C) (34).

### Specificity of PAH2 aptamers

The binding specificity of PAH2 peptide aptamers was assessed as described for PAH1 (Figure 4A). Each of the PAH2 aptamers displayed low level of interaction when retransformed with PAH1, indicating that interaction between PAH2 recovered aptamers and PAH2 was specific.

We have shown previously that introduction of PAH1 residues Val7 and Leu14 at their corresponding position in PAH2 impairs interaction with Mad indicating that PAH2 residues Phe7 and Val14 play an important role in specificity between PAH2 and Mad interaction (29). Therefore, we assumed that PAH2 residues Phe7 and Val14 may also play an important role in the specificity of interaction between PAH2-specific aptamers and PAH2. The interaction between PAH2 and the aptamers was assessed upon mutating

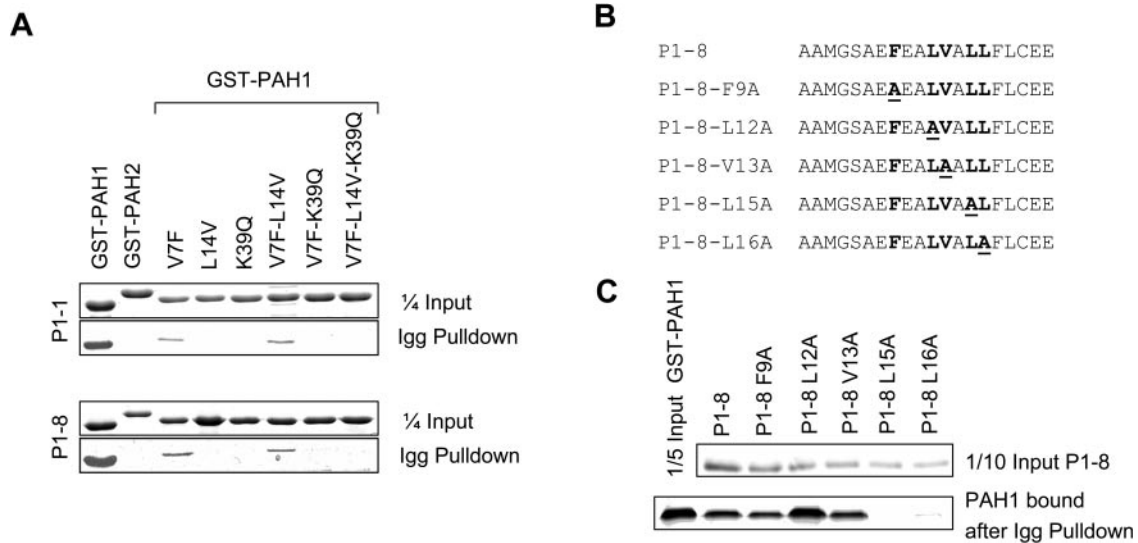


**Figure 3.** Analysis of the interaction between PAH1 and the FXXLVXLL motif *in vitro*. (A) Igg pull-down of P1-1 and P1-8. P1-1 and P1-8 were fused to ProtG and incubated with GST fused to PAH1, PAH2, PAH1 single, double or triple mutant V7F, L14V and K39Q and washed extensively. Bound material was eluted, separated on SDS-PAGE and stained using coomassie blue. (B) Alanine scan strategy. Every established mutants used are shown. (C) Igg pull-down of FXXLVXLL mutants of P1-8. Every mutant of P1-8 were fused to ProtG and incubated with GST-PAH1. Bound material was eluted, separated on SDS-PAGE and stained using coomassie blue. Upper panel depicts input of the different P1-8 mutants used while lower panel depicts the GST-PAH1 bound fraction after Igg pull-down.

conserved PAH2 residues Phe7 and Val14 to the corresponding PAH1 residues Val7 and Leu14. F7V or L14V substitutions in PAH2 affected binding of most aptamers apart from P2-7 and P2-11 (Figure 4B). The double PAH2 mutant F7V V14L failed to interact with any of the aptamers except P2-7. These results thus corroborate and extend the importance of these PAH2 residues for the interaction with Mad to other PAH2 interacting aptamers (29).

Two striking observations were made upon visual inspection of the PAH2 aptamer sequences. First, the strongest PAH2 aptamer P2-2 shows homology to sequences of the PAH2 SIDs from Pf1 and Mad family members. Second, P2-3, P2-11 and P2-6 share a A[AV]X[VA][LV] motif and show homology to SIDs from TIEG1 and TIEG2, Ume6, HBP1 and BTEB4 (Figure 4C). This suggests that the PAH2 domain of Sin3 can recruit two types of SIDs, Mad-like high-affinity SIDs and moderate affinity SIDs with a A[AV]X[VA][LV] motif.

#### Purification of TAP-tagged mSin3b and association with NRL

Although a few peptide aptamers displayed homology to the putative PAH2 interactors BTB5 and a BTB/POZ domain containing protein 12 (Figure 4C), we embarked on a different but complementary experimental strategy to identify Sin3 interacting proteins by purifying a TAP-tagged Sin3b complex from HEK 293 cells. Analysis of the purified Sin3b complex by silver stain showed several bands which were absent from a control purification using extract from wild-type cells. To identify the composition of the Sin3b complex preparation, nano LC-FT-ICR MS analysis was performed (Figure 5A). As judged from % sequence coverage and number of peptides per protein, HDAC1, HDAC2 and Sin3b were present at stoichiometric levels whereas

the histone-binding proteins RbAp46/48, HDAC1-binding protein SDS3, RBP1, SAP130, breast cancer metastasis suppressor BRMS1 and Sin3a were present in sub-stoichiometric amounts (Figure 5B). These results suggest that we purified a Sin3b sub-complex composed exclusively of Sin3b and HDAC1/2 as well as a complete complex composed of Sin3a, HDAC1/2 and the other known subunits. FT-MS (Fourier transform-ion cyclotron resonance-mass spectroscopy) analysis also revealed mono-methylation on K386 of mSin3b, a conserved lysine residue localized in the SDS3/HDAC interaction domain (Figure 5C).

In addition to proteins that are part of the Sin3/HDAC complex, peptides matching the transcription factors Pf1 and Mad1 were identified that are known to interact with the Sin3/HDAC complex. Thus this new tagging/proteomic procedure can be used to identify interacting transcription factors. NRL, a known transcription factor was also detected in the FT-MS analysis, suggesting that it interacts with the Sin3/HDAC complex. Visual inspection of the NRL amino acid sequence revealed a short predicted  $\alpha$  helical stretch with a striking homology to aptamer P2-11 suggesting that NRL and the PAH2 domain of Sin3b may indeed interact (Figure 5D). To directly test an interaction between PAH2 and NRL, GST pull-down experiments were performed. Extracts derived from cells transfected with myc-tagged NRL were incubated with equal amounts of GST-PAH2 or GST-PAH1 and GST beads. A specific interaction between NRL and GST-PAH2, but not with GST-PAH1, could be detected, providing biochemical evidence for a direct interaction between NRL and the PAH2 domain of mSin3b (Figure 5E).

Finally, we performed reporter assays to assess the functional role of NRL region 125–150 in transcription. We transfected the 293 HEK cells with GAL4 fused to NRL or NRL region 125–150 in combination with a *luciferase* reporter

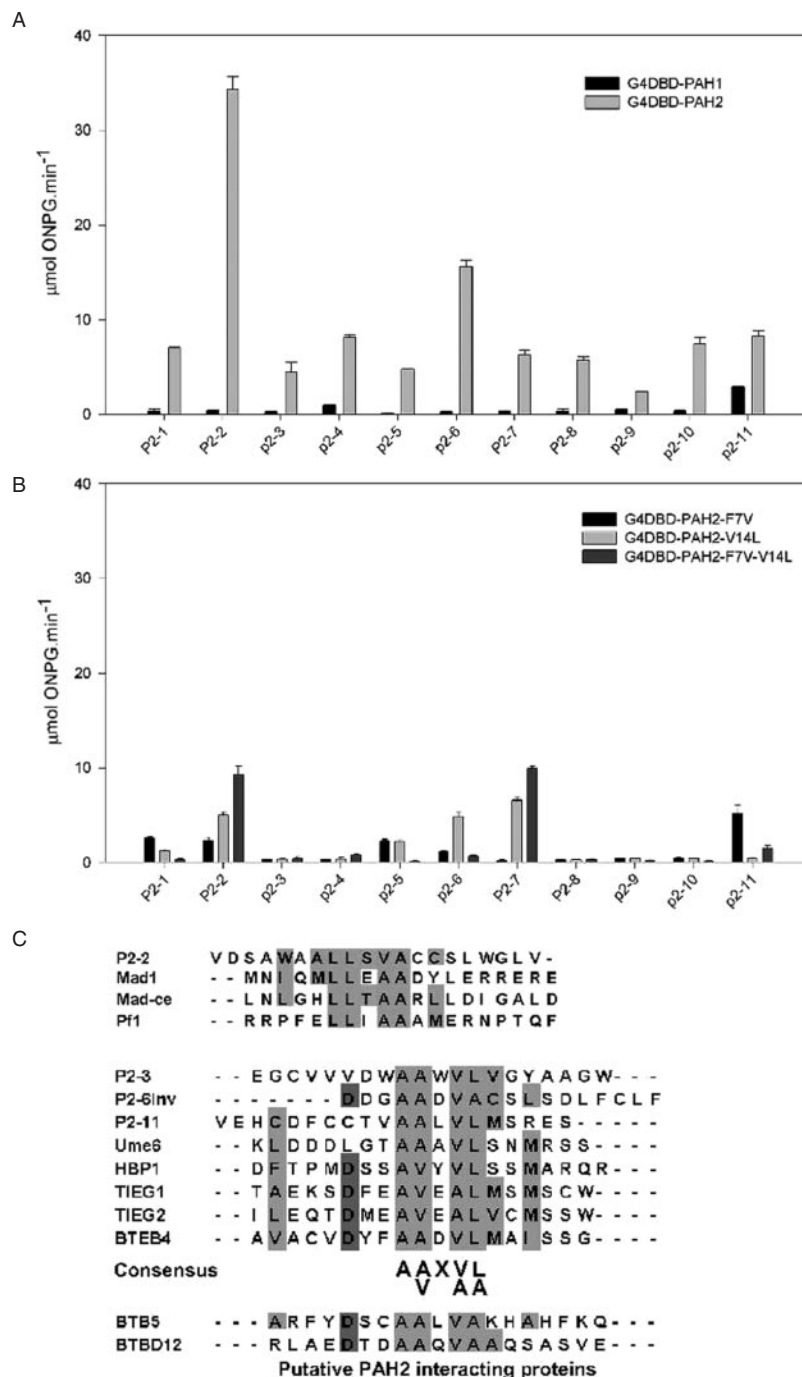


**Figure 4.** Analysis of the interaction of PAH2 aptamers. (A) PAH2 aptamers fused to G4AD were assayed in liquid culture to examine  $\beta$ -galactosidase activity either in the presence G4DBD fused to PAH1 and PAH2. (B)  $\beta$ -Galactosidase assay of PAH2 aptamers in the presence of G4DBD fused to PAH2 single or double mutant F7V and V14L. (C) Sequence alignment of P2-2 and P2-5 showing homology to the SID of Mad, Mad from *Caenorhabditis elegans* and Pf1 (upper panel) Sequence alignment of P2-3, P2-6 inverted sequence and P2-11 matching the A[AV]X[VA][LV] motif conserved in Ume6, HBP1, BTEB4, TIEG1 and TIEG2 SIDs (middle panel). SID from potential PAH2 interacting proteins matching the A[AV]X[VA][LV] motif include residues 65–58 from BTB and kelch domain containing protein 5 (accession no. Q96NJ5) include residues 1070–1063 from BTB/POZ domain containing protein 12 (accession no. Q81Y92) (lower panel).

plasmid containing five GAL4-binding sites. NRL transactivated the reporter gene in our settings in agreement with other reports (Figure 5F) (30). In contrast, NRL region 125–150 has a reproducible repressed expression through the domain that can bind to the Sin3b complex. One

prediction from these observations is that if Sin3b is involved in repression, then the repression should be HDAC-activity dependent. Therefore, we assessed the effect of TSA, a specific inhibitor of HDAC activity on repression. Whereas a modest gain in transcriptional activity of full-length NRL

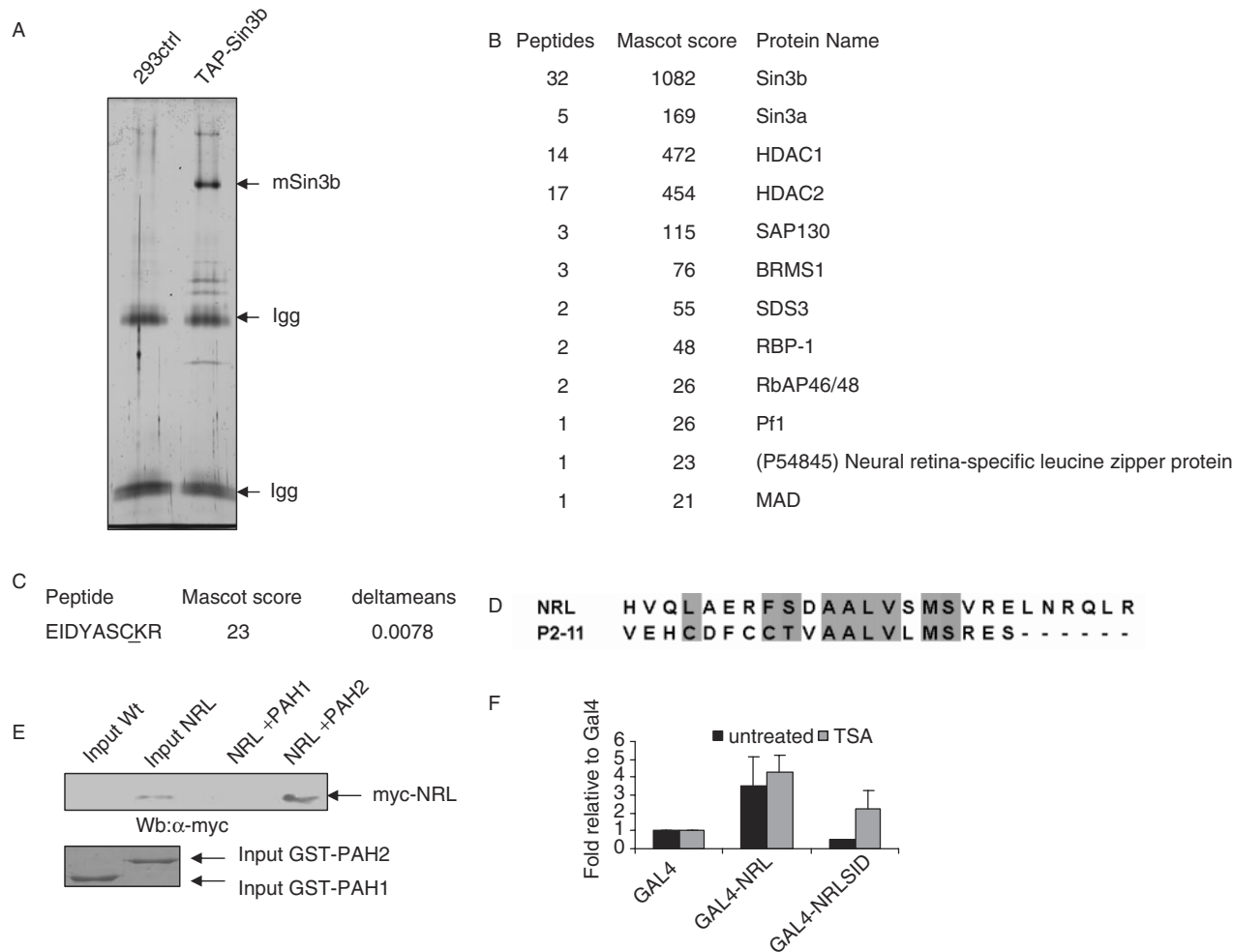


**Figure 5.** TAP-tagging purification of mSin3b and FT/MS analyses reveals NRL as a new PAH2 interacting protein. Stable cell line, TAP-tagging procedure and FT/MS analysis have been described in another study (32). (A) Silver stained gel of purified mSin3b complex from HEK 293 cells. mSin3b is indicated with an arrow. (B) FT-MS/MS analysis with all identified proteins and their respective peptide numbers and Mascot score. (C) FT-MS/MS profile of mSin3b peptide with methylation on K386. (D) Sequence alignment of putative PAH2 SIDs of NRL (residues 125–150) with P2-11. (E) Western blot of a GST pull-down experiment using myc-NRL, GST-PAH1 and GST-PAH2. After extensive washing, bound material was eluted, separated on SDS-PAGE and subjected to western blotting using  $\alpha$ -myc antibody. Lower panel depicts input from GST-PAH1 and GST-PAH2 used in this experiment on a SDS-PAGE and stained using coomassie blue. (F) Reporter assays in 293 HEK cells. GAL4, GAL4-NRL or GAL4-NRL 125–150 were co-transfected with a firefly luciferase reporter under the control of five GAL4-binding sites and a control *Renilla* luciferase plasmid. Ratio between firefly and *Renilla* luciferase activities was expressed in fold relative to Gal4. Average and standard deviation of two experiments performed in duplicate are shown.

could be observed upon TSA treatment, significant derepression by the NRL region 125–150 was observed suggesting that the NRL region 125–150 does indeed associate with HDAC to repress transcription.

In conclusion, the experiments described in this study establish one interaction motif for PAH1 and two different motifs for the PAH2 domain of the Sin3 transcriptional co-repressor and revealed NRL as a novel Sin3 interacting protein.

## DISCUSSION

In this study we have used two different approaches to identify PAH1 and PAH2 interacting proteins. By performing a yeast two-hybrid screening of a peptide aptamer library we have identified a small repertoire of peptides interacting

specifically either the PAH1 or PAH2 domain of mSin3b. Two high-affinity PAH1-binding aptamers contained an LVXLL motif. Very recently, a study by Shio *et al.* (34) revealed Sap25 as a new PAH1 interacting protein part of the Sin3 complex (34). The Sin3 interacting region of Sap25 contains an LXXLL motif with striking similarity to the sequence of PAH1 aptamer identified in this study (Figure 2C). Our findings thus corroborate and extend the importance of the LXXLL motif for Sin3 recruitment.

Three PAH2-binding aptamers shared an A[AV]X[VA][LV] motif included in Ume6 or Kruppel-like family members. One high-affinity PAH2-binding aptamer contained an LLXXA motif shown previously to be part of the SID of Mad family members. A search with the A[AV]X[VA][LV] motif yielded the BTB and kelch containing protein 5 (BKLHD5) and the BTB-POZ domain containing protein

12. Our results therefore suggest that BTB containing proteins could potentially have a repressive function on transcription through recruitment of the Sin3/HDAC complex. Additional studies are required to test this prediction.

We had shown previously that introduction of PAH2 contact residues Phe7, Val14 and Gln39 at their corresponding position in PAH1 enabled a specific interaction with Mad, a PAH2 interacting protein (29). We therefore hypothesized that PAH1 residues Val7, Leu14 and Lys39 play an important role in the specificity between PAH1 and PAH1 aptamers. Conversely we hypothesized that PAH2 residues Phe7, Val14 and Gln39 play an important role in the specificity between PAH2 and PAH2 aptamers. The majority of the identified PAH1 aptamers were indeed affected in their interaction with PAH1 when Val14 was introduced. Furthermore the LVXLL-type aptamers were unable to bind to PAH1 upon introduction of Val14 or Gln39. In contrast the majority of PAH2 aptamers were strongly disturbed in their binding when Val7 and Leu14 of PAH1 were introduced into PAH2 as shown previously for the Mad SID. We therefore speculate that residues 7, 14 and 39 indeed play a determining role in the specificity of interactions between PAH1 and PAH2 and their respective interacting partners.

In a complementary approach to identify novel Sin3 interacting proteins, we purified TAP-tagged mSin3b complex stably expressed in HEK 293 cells and identified known Sin3 complex subunits. We observed co-purification of Sin3a, SDS3, RBP1 and SAP130. The approach also yielded the co-purification of several transcription factors, such as Mad and Pfl as well as a novel protein, NRL zipper protein. Mad and Pfl are known Sin3 PAH2 interactors whereas NRL a bZip transcription factor involved in the regulation of rhodopsin gene activity had not been linked previously to Sin3-dependent repression. Interestingly, reporter assays have shown that amino acids 30–93 of NRL encompass a minimal transactivation domain and that this domain has a substantially higher activation potential than full-length NRL or a fragment encompassing amino acids 30–143. These results described previously suggested that amino acids 93–143 can affect the degree of NRL transactivation (30). Our observations that NRL can interact directly with PAH2 and that the NRL regions 125–150 have HDAC-dependent repressive activity are in line with a model in which Sin3b is involved in regulation of gene expression by NRL.

In conclusion we identified two interaction motifs for the PAH2 domain, a Mad-like motif and an A[AV]X[VA][LV] motif. We also identified one LVXLL-containing motif for the interaction with the PAH1 domain. We reveal that one PAH2 aptamer shows homology to a novel protein NRL zipper which was identified using TAP-tagging purification of mSin3b. Finally we show that the specificity of the identified aptamers for an interaction with either the PAH1 or PAH2 domain depends upon the amino acids at positions 7, 14 and 39 of PAH1 and PAH2, respectively. Thus, this study provides new insights into the molecular determinants of the specificity of PAH1 and PAH2 for their interacting partners. Unravelling the structure of the PAH1 domain in complex with their natural binding partner and elucidation of the specificities of alpha helical motifs ultimately will help to further uncover the molecular basis of specific Sin3 complex formation.

## ACKNOWLEDGEMENTS

We thank Dr K. Butz and Dr F. Hoppe-Seyler for providing us with the aptamer library and the yeast two-hybrid strain and plasmids. We thank Annand Swaroop for providing us with the pcDNA4-NRL plasmid. Special thanks to Dr E. Lasonder for GST-PAH1, GST-PAH2 protein and expertise in mass spectrometry. This work was supported by a grant from The Netherlands Proteomic Centre (NPC). Funding to pay the Open Access publication charges for this article was provided by NPC.

*Conflict of interest statement.* None declared.

## REFERENCES

- Turner,B.M. (2002) Cellular memory and the histone code. *Cell*, **111**, 285–291.
- Jenuwein,T. and Allis,C.D. (2001) Translating the histone code. *Science*, **293**, 1074–1080.
- Cosma,M.P. (2002) Ordered recruitment: gene-specific mechanism of transcription activation. *Mol. Cell*, **10**, 227–236.
- Grozinger,C.M. and Schreiber,S.L. (2002) Deacetylase enzymes: biological functions and the use of small-molecule inhibitors. *Chem. Biol.*, **9**, 3–16.
- Hassig,C.A., Fleischer,T.C., Billin,A.N., Schreiber,S.L. and Ayer,D.E. (1997) Histone deacetylase activity is required for full transcriptional repression by mSin3A. *Cell*, **89**, 341–347.
- Laherty,C.D., Yang,W.M., Sun,J.M., Davie,J.R., Seto,E. and Eisenman,R.N. (1997) Histone deacetylases associated with the mSin3 corepressor mediate mad transcriptional repression. *Cell*, **89**, 349–356.
- Zhang,Y., Sun,Z.W., Iratni,R., Erdjument-Bromage,H., Tempst,P., Hampsey,M. and Reinberg,D. (1998) SAP30, a novel protein conserved between human and yeast, is a component of a histone deacetylase complex. *Mol. Cell*, **1**, 1021–1031.
- Alland,L., David,G., Shen-Li,H., Potes,J., Muhle,R., Lee,H.C., Hou,H., Jr, Chen,K. and DePinho,R.A. (2002) Identification of mammalian Sds3 as an integral component of the Sin3/histone deacetylase corepressor complex. *Mol. Cell Biol.*, **22**, 2743–2750.
- Fleischer,T.C., Yun,U.J. and Ayer,D.E. (2003) Identification and characterization of three new components of the mSin3A corepressor complex. *Mol. Cell Biol.*, **23**, 3456–3467.
- Vermeulen,M., Carrozza,M.J., Lasonder,E., Workman,J.L., Logie,C. and Stunnenberg,H.G. (2004) *In vitro* targeting reveals intrinsic histone tail specificity of the Sin3/histone deacetylase and N-CoR/SMRT corepressor complexes. *Mol. Cell Biol.*, **24**, 2364–2372.
- Meehan,W.J., Samant,R.S., Hopper,J.E., Carrozza,M.J., Shevde,L.A., Workman,J.L., Eckert,K.A., Verderame,M.F. and Welch,D.R. (2004) Breast cancer metastasis suppressor 1 (BRMS1) forms complexes with retinoblastoma-binding protein 1 (RBP1) and the mSin3 histone deacetylase complex and represses transcription. *J. Biol. Chem.*, **279**, 1562–1569.
- Wang,H., Clark,I., Nicholson,P.R., Herskowitz,I. and Stillman,D.J. (1990) The *Saccharomyces cerevisiae* SIN3 gene, a negative regulator of HO, contains four paired amphipathic helix motifs. *Mol. Cell Biol.*, **10**, 5927–5936.
- Wagner,C., Dietz,M., Wittmann,J., Albrecht,A. and Schuller,H.J. (2001) The negative regulator Opi1 of phospholipid biosynthesis in yeast contacts the pleiotropic repressor Sin3 and the transcriptional activator Ino2. *Mol. Microbiol.*, **41**, 155–166.
- Yochum,G.S. and Ayer,D.E. (2001) Pfl, a novel PHD zinc finger protein that links the TLE corepressor to the mSin3A-histone deacetylase complex. *Mol. Cell Biol.*, **21**, 4110–4118.
- Naruse,Y., Aoki,T., Kojima,T. and Mori,N. (1999) Neural restrictive silencer factor recruits mSin3 and histone deacetylase complex to repress neuron-specific target genes. *Proc. Natl Acad. Sci. USA*, **96**, 13691–13696.
- Nagy,L., Kao,H.Y., Chakravarti,D., Lin,R.J., Hassig,C.A., Ayer,D.E., Schreiber,S.L. and Evans,R.M. (1997) Nuclear receptor repression mediated by a complex containing SMRT, mSin3A, and histone deacetylase. *Cell*, **89**, 373–380.

17. Heinzel, T., Lavinsky, R.M., Mullen, T.M., Soderstrom, M., Laherty, C.D., Torchia, J., Yang, W.M., Brard, G., Ngo, S.D., Davie, J.R. *et al.* (1997) A complex containing N-CoR, mSin3 and histone deacetylase mediates transcriptional repression. *Nature*, **387**, 43–48.
18. Washburn, B.K. and Esposito, R.E. (2001) Identification of the Sin3-binding site in Ume6 defines a two-step process for conversion of Ume6 from a transcriptional repressor to an activator in yeast. *Mol. Cell. Biol.*, **21**, 2057–2069.
19. Zhang, J.S., Moncrieffe, M.C., Kaczynski, J., Ellenrieder, V., Prendergast, F.G. and Urrutia, R. (2001) A conserved alpha-helical motif mediates the interaction of Sp1-like transcriptional repressors with the corepressor mSin3A. *Mol. Cell. Biol.*, **21**, 5041–5049.
20. Ayer, D.E., Lawrence, Q.A. and Eisenman, R.N. (1995) Mad-Max transcriptional repression is mediated by ternary complex formation with mammalian homologs of yeast repressor Sin3. *Cell*, **80**, 767–776.
21. Ayer, D.E., Laherty, C.D., Lawrence, Q.A., Armstrong, A.P. and Eisenman, R.N. (1996) Mad proteins contain a dominant transcription repression domain. *Mol. Cell. Biol.*, **16**, 5772–5781.
22. Schreiber-Agus, N., Chin, L., Chen, K., Torres, R., Rao, G., Guida, P., Skoultschi, A.I. and DePinho, R.A. (1995) An amino-terminal domain of Mx1 mediates anti-Myc oncogenic activity and interacts with a homolog of the yeast transcriptional repressor SIN3. *Cell*, **80**, 777–786.
23. Swanson, K.A., Knoepfler, P.S., Huang, K., Kang, R.S., Cowley, S.M., Laherty, C.D., Eisenman, R.N. and Radhakrishnan, I. (2004) HBP1 and Mad1 repressors bind the Sin3 corepressor PAH2 domain with opposite helical orientations. *Nature Struct. Biol.*, **11**, 738–746.
24. Eilers, A.L., Billin, A.N., Liu, J. and Ayer, D.E. (1999) A 13-amino acid amphipathic alpha-helix is required for the functional interaction between the transcriptional repressor Mad1 and mSin3A. *J. Biol. Chem.*, **274**, 32750–32756.
25. Spronk, C.A., Tessari, M., Kaan, A.M., Jansen, J.F., Vermeulen, M., Stunnenberg, H.G. and Vuister, G.W. (2000) The Mad1–Sin3B interaction involves a novel helical fold. *Nature Struct. Biol.*, **7**, 1100–1104.
26. van-Ingen, H., Lasonder, E., Jansen, J.F., Kaan, A.M., Spronk, C.A., Stunnenberg, H.G. and Vuister, G.W. (2004) Extension of the binding motif of the Sin3 interacting domain of the Mad family proteins. *Biochemistry*, **43**, 46–54.
27. Brubaker, K., Cowley, S.M., Huang, K., Loo, L., Yochum, G.S., Ayer, D.E., Eisenman, R.N. and Radhakrishnan, I. (2000) Solution structure of the interacting domains of the Mad–Sin3 complex: implications for recruitment of a chromatin-modifying complex. *Cell*, **103**, 655–665.
28. Pang, Y.P., Kumar, G.A., Zhang, J.S. and Urrutia, R. (2003) Differential binding of Sin3 interacting repressor domains to the PAH2 domain of Sin3A. *FEBS Lett.*, **548**, 108–112.
29. Le-Guezennec, X., Vriend, G. and Stunnenberg, H.G. (2004) Molecular determinants of the interaction of Mad with the PAH2 domain of mSin3. *J. Biol. Chem.*, **279**, 25823–25829.
30. Friedman, J.S., Khanna, H., Swain, P.K., Denicola, R., Cheng, H., Mitton, K.P., Weber, C.H., Hicks, D. and Swaroop, A. (2004) The minimal transactivation domain of the basic motif-leucine zipper transcription factor NRL interacts with TATA-binding protein. *J. Biol. Chem.*, **279**, 47233–47241.
31. Spronk, C.A., Jansen, J.F., Tessari, M., Kaan, A.M., Aelen, J., Lasonder, E., Stunnenberg, H.G. and Vuister, G.W. (2001) Sequence-specific assignment of the PAH2 domain of Sin3B free and bound to Mad1. *J. Biomol. NMR*, **19**, 377–378.
32. Le Guezennec, X., Vermeulen, M., Brinkman, A.B., Hoeijmakers, W., Cohen, A., Lasonder, E. and Stunnenberg, H.G. (2005) MBD2/NuRD and MBD3/NuRD, Two Distinct Complexes with Different Biochemical and Functional Properties. *Mol. Cell. Biol.*, **26**, 843–851.
33. Butz, K., Denk, C., Ullmann, A., Scheffner, M. and Hoppe-Seyler, F. (2000) Induction of apoptosis in human papillomaviruspositive cancer cells by peptide aptamers targeting the viral E6 oncoprotein. *Proc. Natl Acad. Sci. USA*, **97**, 6693–6697.
34. Shiiio, Y., Rose, D.W., Aur, R., Donohoe, S., Aebersold, R. and Eisenman, R.N. (2006) Identification and characterization of SAP25, a novel component of the mSin3 corepressor complex. *Mol. Cell. Biol.*, **26**, 1386–1397.